Malaysian Journal of Chemistry, 2026, Vol. 28(1), 422-433
(Special Issue: *12th International Conference of the College of Science & 3rd Conference of Chemistry Department 2025*)

Synthesis of Pyridinium Derivatives as Corrosion Inhibitors for Mild Steel in Acidic Solution

Baraa Watheq Hachim* and Mehdi Salih Shihab
Department of Chemistry, College of Science, Al-Nahrain University, Baghdad, Iraq
*Corresponding author (e-mail: alamiribara@gmail.com)

In this study, the inhibitory performances of three pyridinium bromide derivatives, namely 1-benzyl-4-((3-(4-chlorobenzylidene)-2-oxocyclohexylidene)methyl)pyridin-1-ium bromide, **C1**; 4-((3-(4-chlorobenzylidene)-2-oxocyclohexylidene)methyl)-1-(2-oxopropyl)pyridin-1-ium bromide, **C2**; 4-((3-(4-chlorobenzylidene)-2-oxocyclohexylidene)methyl)-1-(2-oxo-2-phenylethyl)pyridin-1-ium bromide, **C3**, were investigated for mild steel corrosion in 1 M H_2SO_4 for 24 hours at 25˚C. The evaluation was conducted using the weight loss technique, while the molecular structures were confirmed by Proton Nuclear Magnetic Resonance (^{1}H-NMR) and Fourier Transform Infrared (FT-IR) Spectroscopy. The results showed that the inhibition efficiency (IE%) of all three compounds was strong and improved gradually as the inhibitor concentration increased. This improvement was attributable to increased adsorption of inhibitor molecules on the mild steel surface, resulting in higher surface coverage(θ). At the same time, the rate of corrosion decreased. Furthermore, the adsorption of the studied compounds on the surface of mild steel followed the Langmuir isotherm model, with high K_{ads} values, which supported the substance's better inhibitive activity. The results indicated negative ΔG ads values, signifying that the adsorption of inhibitor molecules on the mild steel surface occurred spontaneously via a combined mechanism of physisorption and chemisorption. These results indicate that pyridinium bromide derivatives can act as promising and effective corrosion inhibitors for mild steel in acidic media.

Keywords: Adsorption, H_2SO_4, metal surface, synthesis, weight loss

Received: September 2025; Accepted: November 2025

Mild steel is regarded as one of the most widely employed engineering materials because of its considerable industrial importance. It is utilized in many sectors, including construction, petroleum extraction and refining, metalworking machinery, chemical industries, and marine infrastructure [1]. Nonetheless, its susceptibility to severe corrosion when exposed to aggressive environments, especially acidic media and chloride-containing solutions, poses a major limitation to its widespread industrial use [2]. In acidic conditions, corrosion often entails the dissolving of iron (Fe) and the generation of iron ions (Fe^{2+}), accompanied by the liberation of hydrogen gas (H_2). The process is affected by variables such as pH, temperature, and the concentration of corrosive agents. Comprehending the essential corrosion mechanisms in mild steel establishes the foundation for formulating efficient corrosion inhibition tactics [3]. Corrosion is an unavoidable process characterized by the irreversible deterioration of metals or alloys due to chemical or electrochemical interactions with their environment. Corrosion inflicts significant damage on metallic resources, leading to health risks and the decline of flora and fauna, including humans, as well as substantial economic impacts globally [4]. Various techniques exist to prevent mild steel (MS) from corrosion, such as micro-arc oxidation, thermal spraying, electroplating, and the utilization of organic coatings [5]. However, the most practical and cost-effective method for preventing mild steel from corrosion in an extremely acidic environment is to employ a specific category of chemical compounds referred to as inhibitors [6]. The application of corrosion inhibitors in corrosive environments efficiently prevents significant damage to metal surfaces caused by corrosion. Corrosion inhibitors demonstrate solubility in water and maintain thermal stability even in highly aggressive acidic conditions. These compounds are capable of interacting with metallic ions to form a metal-inhibitor complex that remains thermally, chemically, and thermodynamically stable, especially in acidic conditions [7]. The resultant complex is efficiently adsorbed onto the metallic surface, forming a stable thin film that functions as a protective barrier, efficiently isolating the metal from the corrosive environment. Consequently, the protective layer offers the metallic surface substantial protection, shielding it efficiently from corrosive processes. The efficacy of corrosion inhibitors is ascribed to their polar functional groups (–SH, –OCH_3, –OH, –NH_2, –C=N–) and heteroatoms like phosphorus, oxygen, sulfur, and nitrogen [8-9]. These properties allow the inhibitor to alter corrosion mechanisms by reducing oxidation on the metal surface and preventing reduction reactions

†Paper presented at the 12th International Conference of the College of Science & 3rd Conference of Chemistry Dept. 2025

at the cathode [10]. The objective of this study is to investigate the corrosion behavior of mild steel in 1M H_2SO_4 at 25˚C in the presence of some pyridinium bromide derivatives using weight loss.

EXPERIMENTAL

Materials:

All of the chemicals were obtained from Macklin, Fluorochem, and BLDpharm and were utilized in their original form.

Techniques:

The melting points of the synthesized compounds were determined using an open capillary method on a Gallenkamp melting point apparatus at the Department of Chemistry, Al-Nahrain University. The infrared (IR) spectra were recorded on a Shimadzu FTIR spectrophotometer within the transmission range of 4000–400 cm^{-1}, with the samples prepared as potassium bromide (KBr) disks at the University of Baghdad. The proton nuclear magnetic resonance (^1H NMR) spectra were obtained using a Bruker 400 MHz spectrometer (Germany), employing tetramethylsilane (TMS) as an internal reference and DMSO-d_6 as the solvent, at the University of Tehran, Iran.

Synthesis of Suggested Inhibitors

Pyridinium bromide derivatives inhibitor, name: namely 1-benzyl-4-((3-(4-chlorobenzylidene)-2-oxocyclohexylidene)methyl)pyridin-1-ium bromide, **C1**; 4-((3-(4-chlorobenzylidene)-2-oxocyclohexylidene) methyl)-1-(2-oxopropyl)pyridin-1-ium bromide, **C2**; 4-((3-(4-chlorobenzylidene)-2-oxocyclohexylidene) methyl)-1-(2-oxo-2-phenylethyl)pyridin-1-ium bromide, **C3**; were synthesized as below:

Synthesis of Chalcone

A mixture of aromatic benzaldehyde (4-chlorobenzaldehyde) (0.01 mol) with cyclohexanone (0.01 mol, 1.04 mL) and an aqueous solution of sodium hydroxide (1 mL, 10%) was added. The mixture was stirred for 2–3 hours in an ice bath. It was then cooled overnight, freezing. Afterward, it was diluted with ice-cold distilled water, filtered, washed several times with cold water, and air-dried. (see **scheme 1**) [11-12].

Synthesis of 2-(4-chlorobenzylidene)-6-(pyridin-4-ylmethylene) Cyclohexan-1-one

A solution of 2-(4-Chlorobenzylidene) cyclohexan-1-one (0.005 mol) was prepared in 10 mL of absolute ethanol. To this, an equimolar amount (0.005 mol) of 4-pyridinecarboxaldehyde was added, followed by 1 mL of 10% sodium hydroxide solution. The reaction mixture was stirred at room temperature for three hours to ensure completion of the condensation process (see Table 1, Scheme 1).

Synthesis of Pyridinium Salts (C1, C2, and C3)

A mixture of 2-(4-chlorobenzylidene)-6-(pyridin-4-ylmethylene) cyclohexan-1-one (0.005 mol) and an equimolar amount (0.005 mol) of the appropriate alkyl halide (benzyl bromide, bromoacetone, or 2-bromoacetophenone) was prepared in 10 mL of ethanol, and the reaction mixture was heated under reflux for 48 hours., (see Table 1, scheme1) [13].

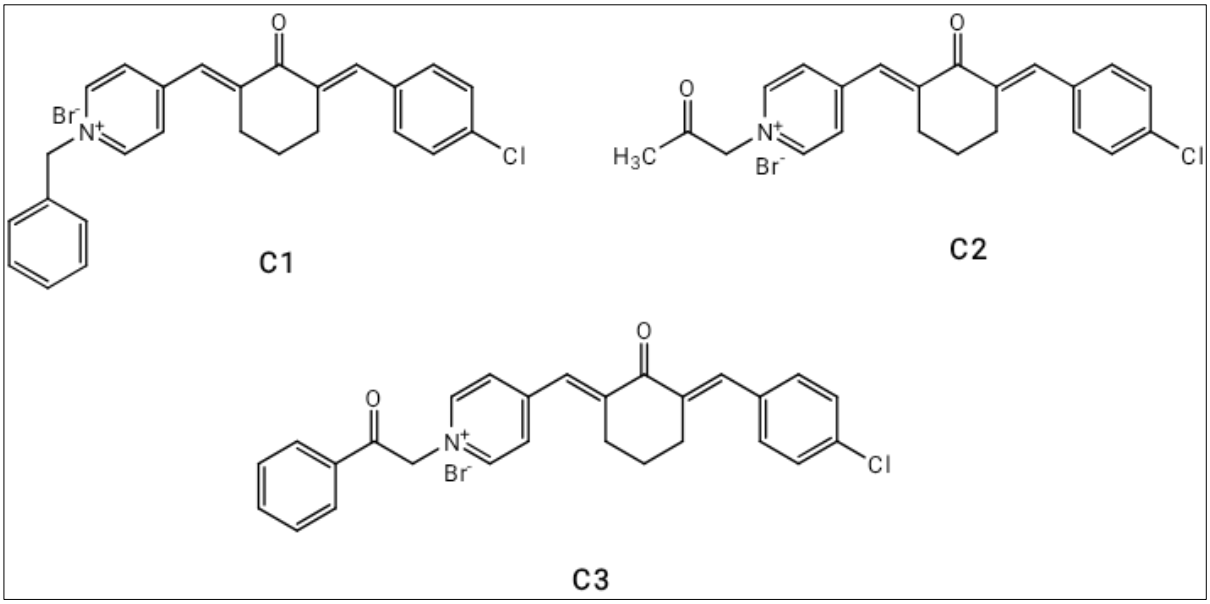

Figure 1. The molecular formula of the suggested inhibitors (C1, C2, and C3).

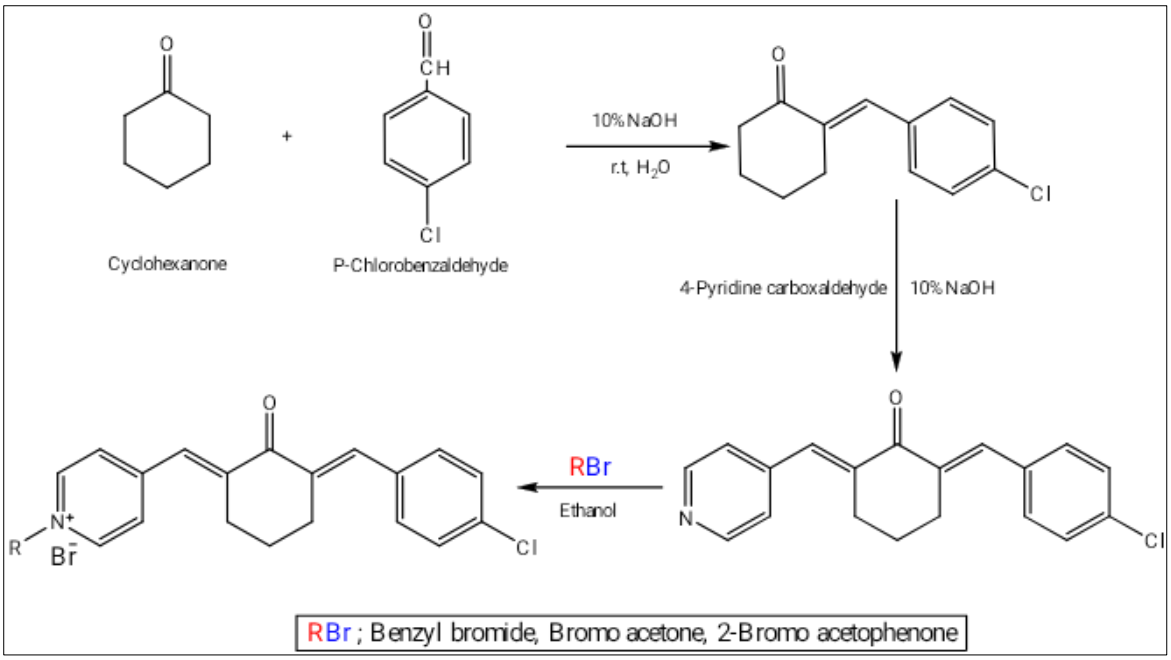

Scheme 1. The pyridinium salts synthesis process (C1, C2, and C3).

Preparation of Solution

A solution of 1M H_2SO_4 was prepared by diluting analytical-grade sulphuric acid (98%) with distilled water. A volumetric flask was used to keep the prepared solution, and it was sealed with a tight stopper. Several inhibitor concentrations (5×10^{-4}, 1×10^{-3}, 5×10^{-3}, and 1×10^{-2}M) were prepared in 1M H_2SO_4, which served as the solvent.

Gravimetric Method

This method was employed to calculate the corrosion rates. The employed sheet of mild steel primarily consists of iron, with the following percentages: 0.002% phosphorus, 0.288% manganese, 0.03% carbon, 0.0154% sulfur, 0.0199% chromium, 0.002% molybdenum, 0.065% copper, and 0.0005% vanadium. Before each experiment, a mild steel specimen with a diameter of 2.5 cm was polished using a sequence of emery papers up to grade 2000. The specimen was then subsequently rinsed with distilled water, ethanol, and acetone, and finally dried at room temperature. After accurate weighing, the samples were submerged in 25 mL of1 M H_2SO_4 solution, both in the absence and in the presence of inhibitors at concentrations of 0.0005, 0.001, 0.005, and 0.01 M. After 24 hours of immersion, the specimens were removed, rinsed with distilled water to eliminate any corrosion products, washed with ethanol, dried, and subsequently reweighed. Mass loss measurements were performed in accordance with the ASTM standard method [14]. The corrosion rate (W) and inhibition efficiency (IE%) were calculated using the following equations [15]:

$$W \frac{\Delta m}{St} \quad (1)$$

Where W represents the corrosion rate of mild steel, Δm is the mass loss in milligrams (mg), S is the surface area in square centimeters (cm^2), and t denotes the immersion time in hours. Inhibition efficiency (IE%) was determined using Equation (2), as shown below [16].

$$IE(\%) = \frac{W_\circ - W}{W_\circ} \times 100 \quad (2)$$

W_o and W are the mild steel corrosion rates, without and with inhibitors, respectively.

Table 1. FTIR spectral data and physical properties of prepared compounds.

Comp.	Name	M.Wt(g/mol)	color	M.p ºC	Yield%	FTIR
1	2-(4-Chlorobenzylidene) cyclohexan-1-one	220.70	Pale yellow	48-50	97	Aliphatic(C-H) 2943, 2862, and aromatic (C-H) 3049, (C=O) 1697, (C=C) 1595
2	*2-(4-chlorobenzylidene)-6-(pyridin-4-ylmethylene) cyclohexan-1-one*	309.79	Yellow	82-84	91	Aliphatic(C-H) 2935, 2864, and aromatic (C-H) 3060, (C=O) 1664, (C=N)1598, (C=C) 1550
C1	1-benzyl-4-((3-(4-chlorobenzylidene)-2-oxocyclohexylidene)methyl) pyridin-1-ium bromide	480.83	Dark brown	116-118	95	Aliphatic(C-H) 2937, 2867, and aromatic (C-H) 3031, (C=O) 1701, (C=N)1635, (C=C) 1602
C2	4-((3-(4-chlorobenzylidene)-2-oxocyclohexylidene) methyl)-1-(2-oxopropyl) pyridin-1-ium bromide	446.77	Reddish brown	94-96	73	Aliphatic(C-H) 2933, 2869, and aromatic (C-H) 3028, Cyclo(C=O) 1668, acetone (C=O) 1710, (C=N) 1637, (C=C) 1602
C3	4-((3-(4-chlorobenzylidene)-2-oxocyclohexylidene) methyl)-1-(2-oxo-2-phenylethyl)pyridin-1-ium bromide	508.84	Brown	132-134	86	Aliphatic(C-H) 2937, 2893, and aromatic (C-H) 3055, Cyclo(C=O) 1660, acetophenone (C=O)1726, (C=N) 1641, (C=C) 1596

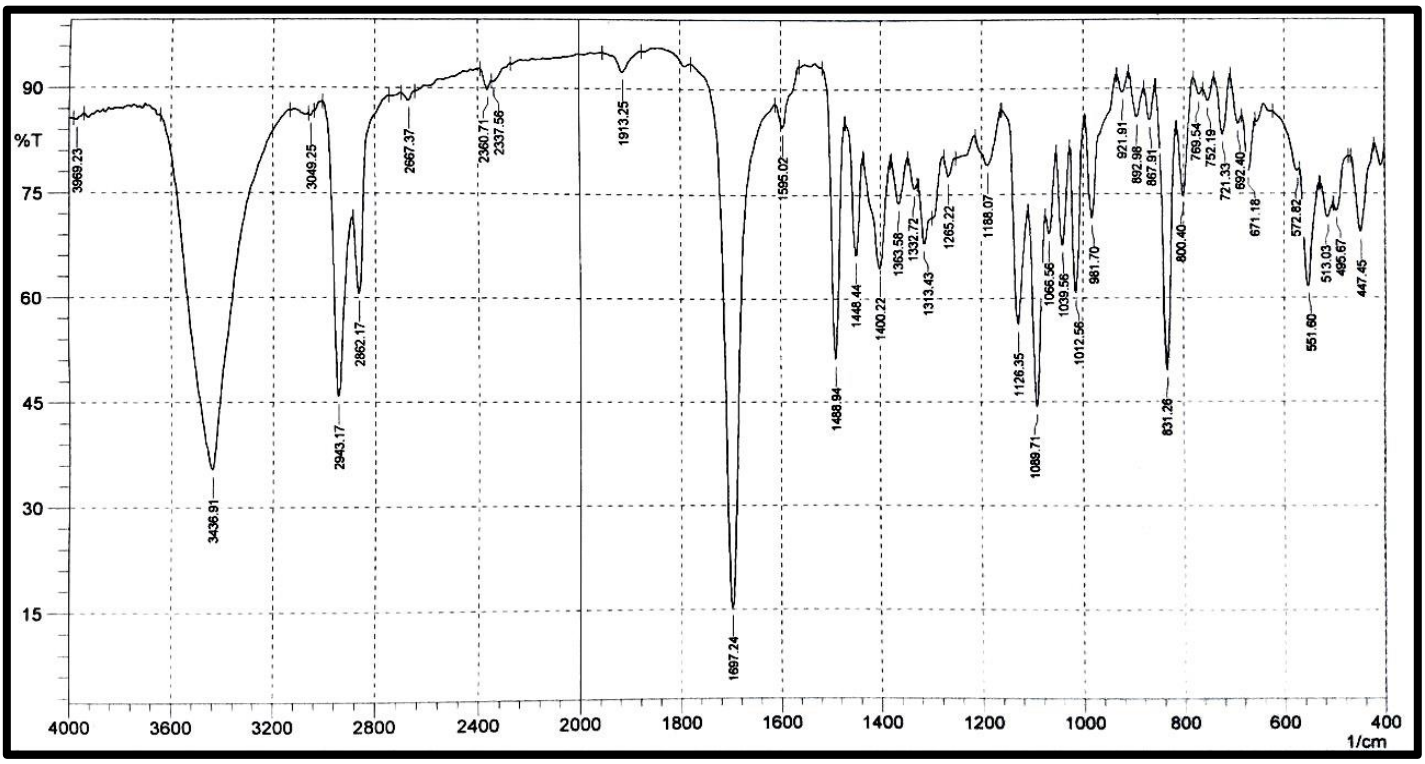

Figure 2. FTIR of 2-(4-Chlorobenzylidene) cyclohexan-1-one.

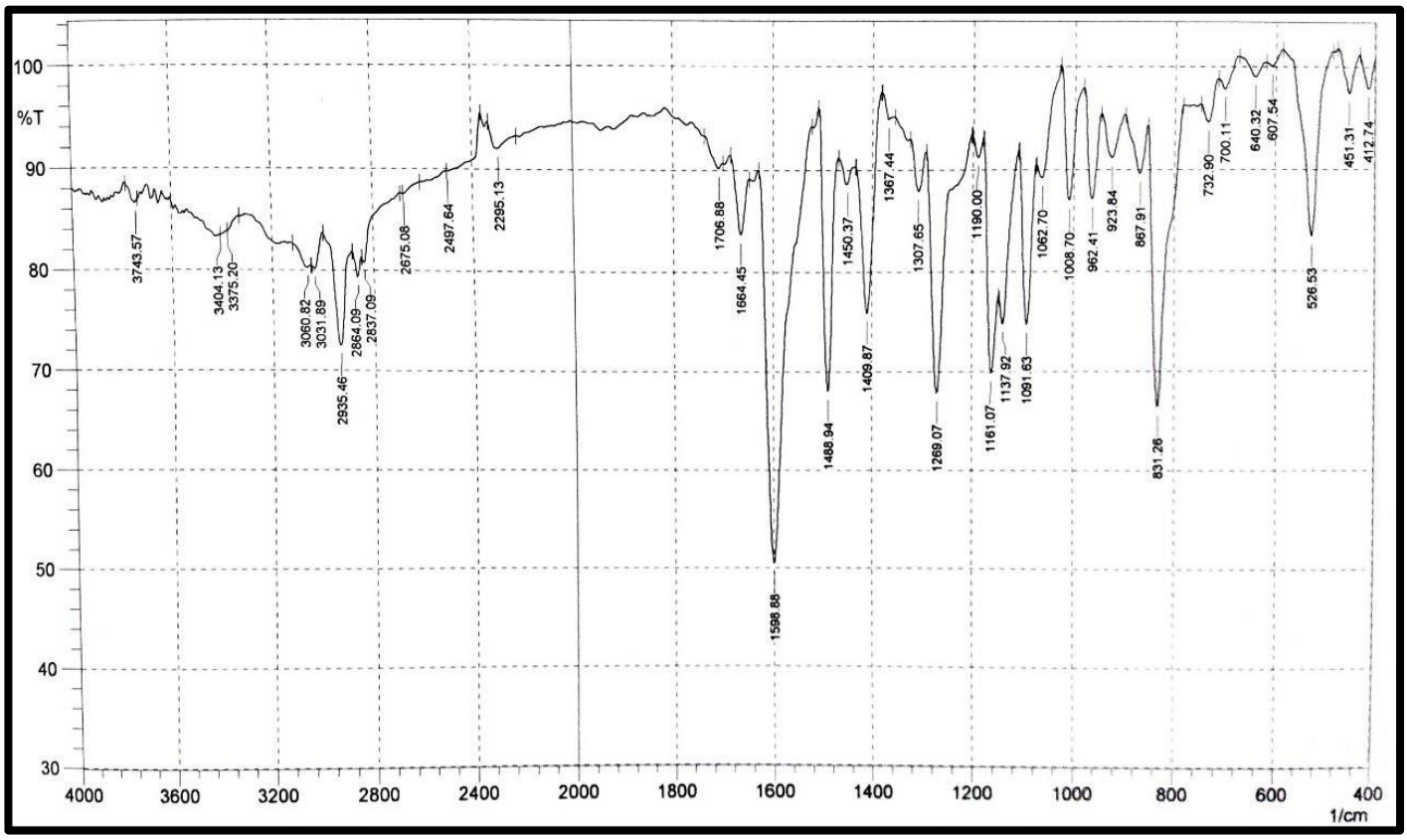

Figure 3. FTIR of *2-(4-chlorobenzylidene)-6-(pyridin-4-ylmethylene) cyclohexan-1-one.*

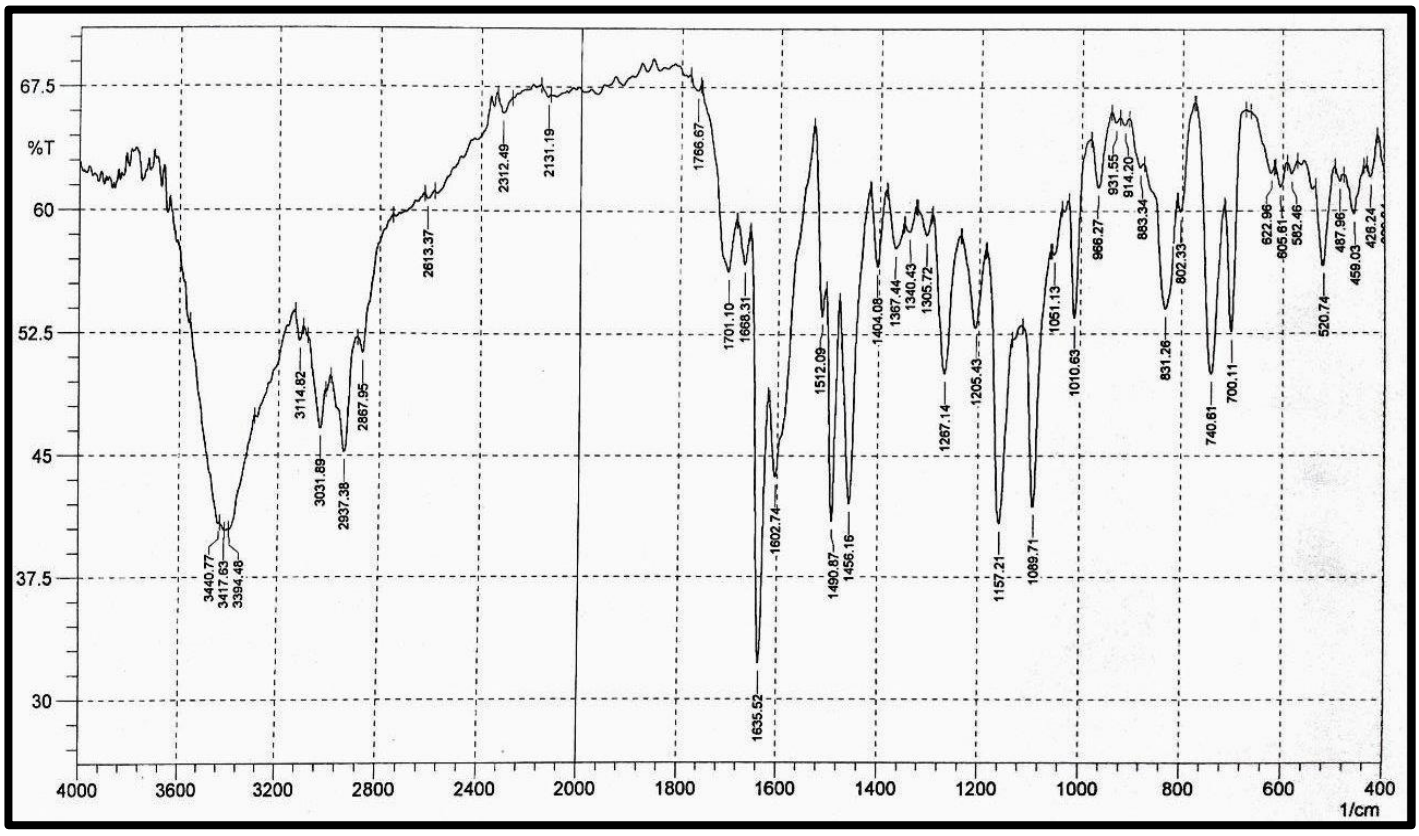

Figure 4. FTIR of Compound (**C1).**

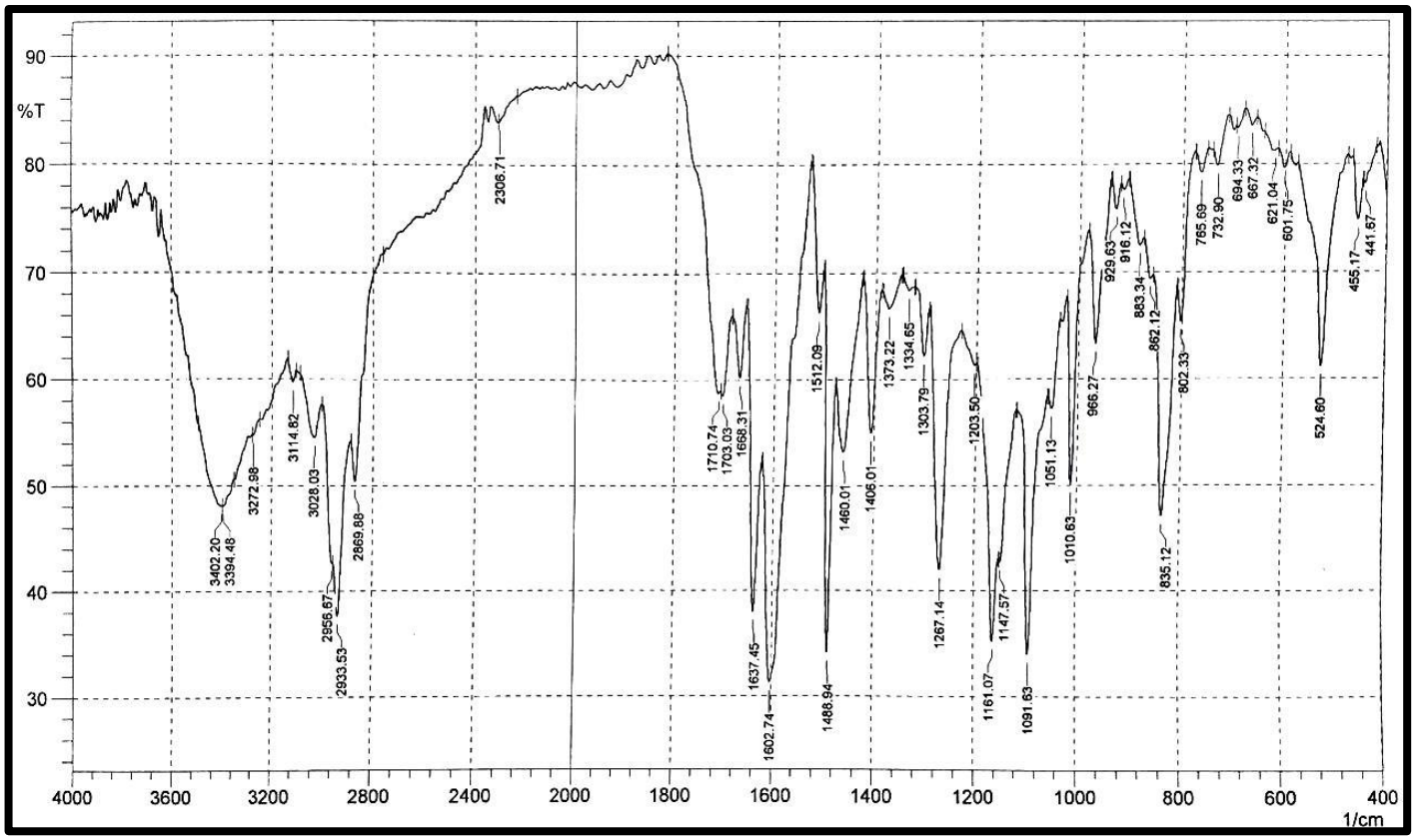

Figure 5. FTIR of Compound (**C2)**.

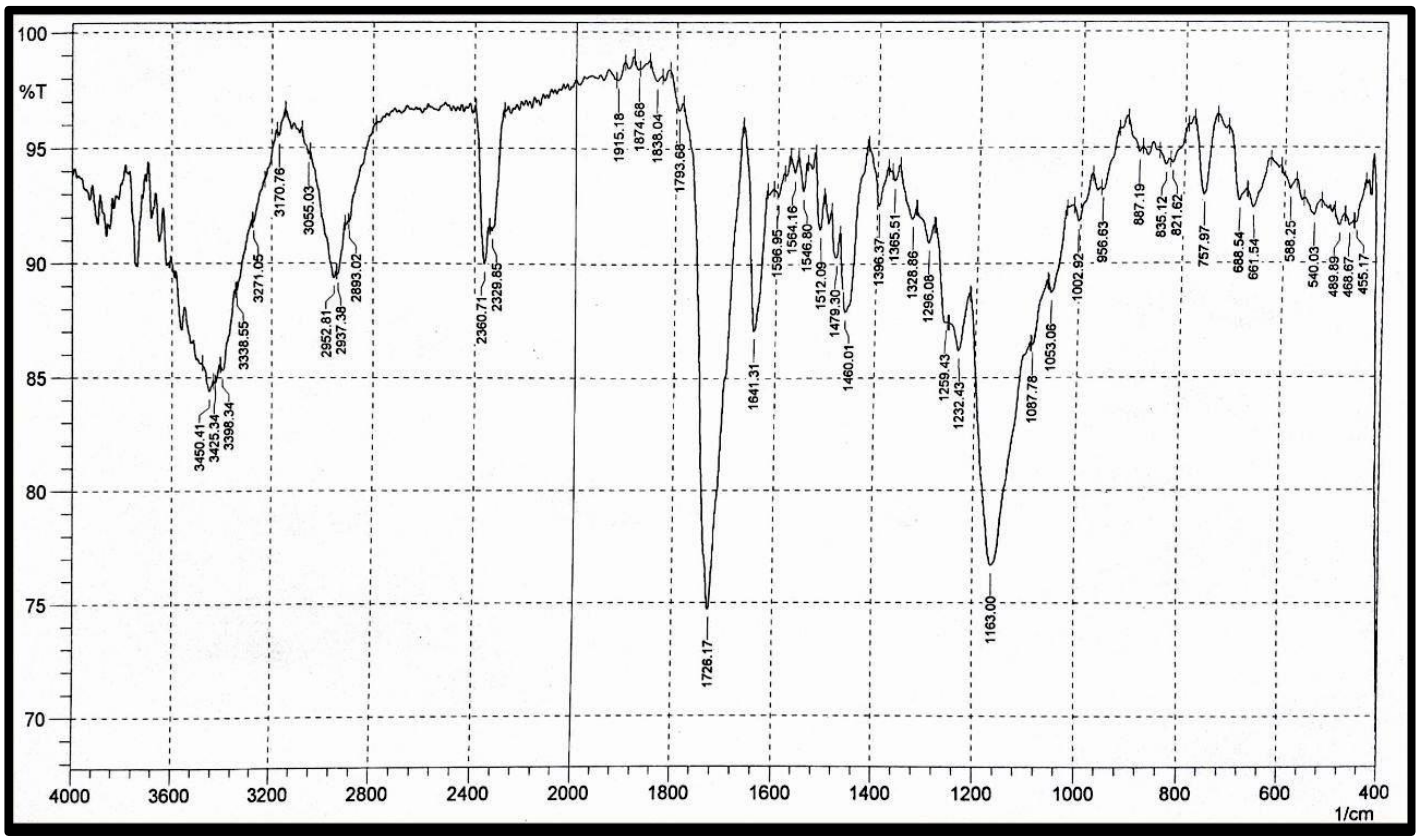

Figure 6. FTIR of Compound (**C3)**.

Table 2. The ^{1}H-NMR spectral data of compounds (C1–C3) in ppm.

Comp. No.	Compound structure	^{1}H-NMR data of (δ-H) in ppm
C1	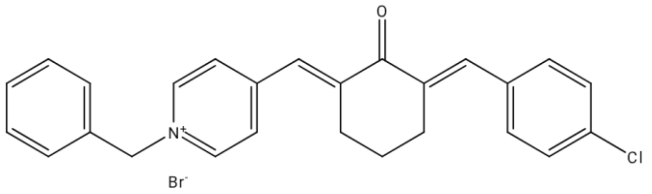	6H of CH_2 of cyclohexanone (1.13-2.89); 4H of pyridine ring (7.9-9.27); 2H of CH_2N^+ group (5.95); 1H of =CH-Ar group(7.36); 9H of aromatic ring (7.43-7.66)
C2	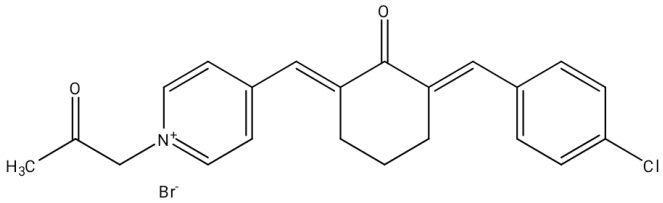	6H of CH_2 of cyclohexanone (1.09-2.84); 3H of $COCH_3$ group(2.86); 2H of CH_2N^+ group (6.51); 1H of =CH-Ar group (7.37); 4H of pyridine ring (7.53-8.6); 4H of aromatic ring(7.40-7.50)
C3	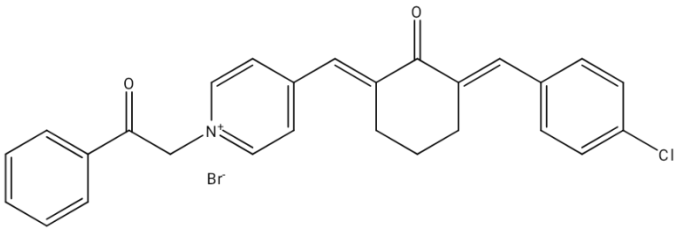	6H of CH_2 of cyclohexanone (1.16-2.89); 2H of CH_2N^+ group (6.51); 1H of =CH-Ar group (7.37); 9H of aromatic ring (7.50-8.9); 4H of pyridine ring (7.94-9.06)

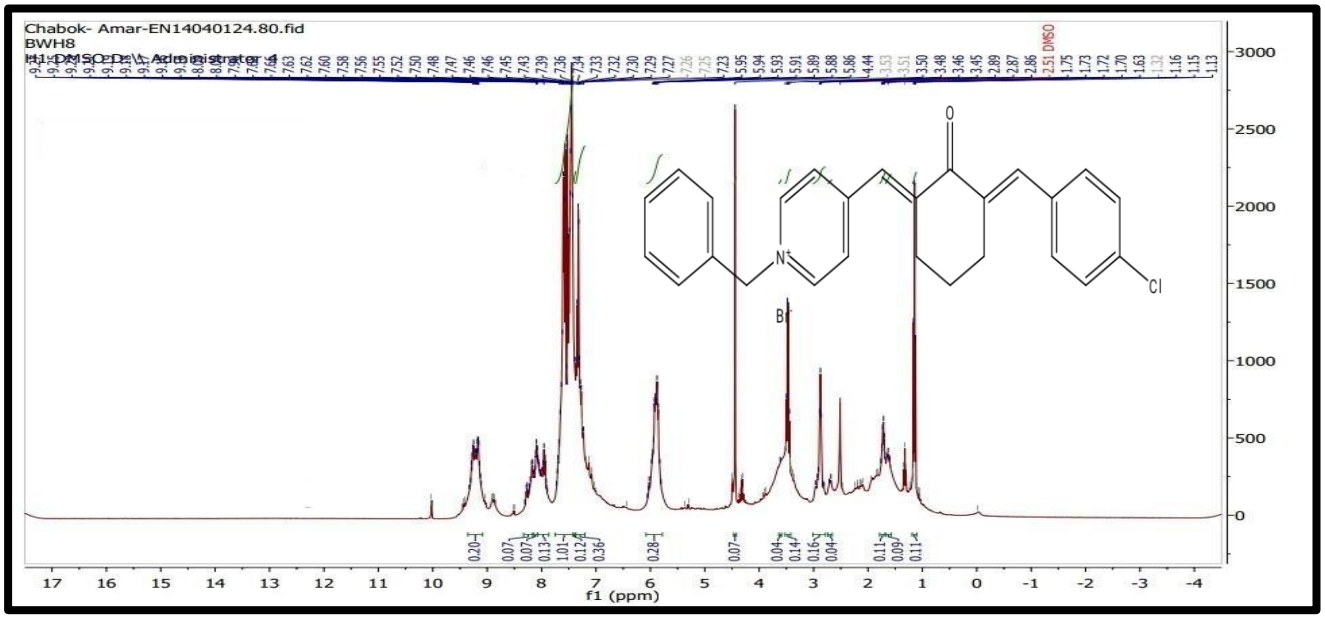

Figure 7. ^{1}H-NMR of compound (C1).

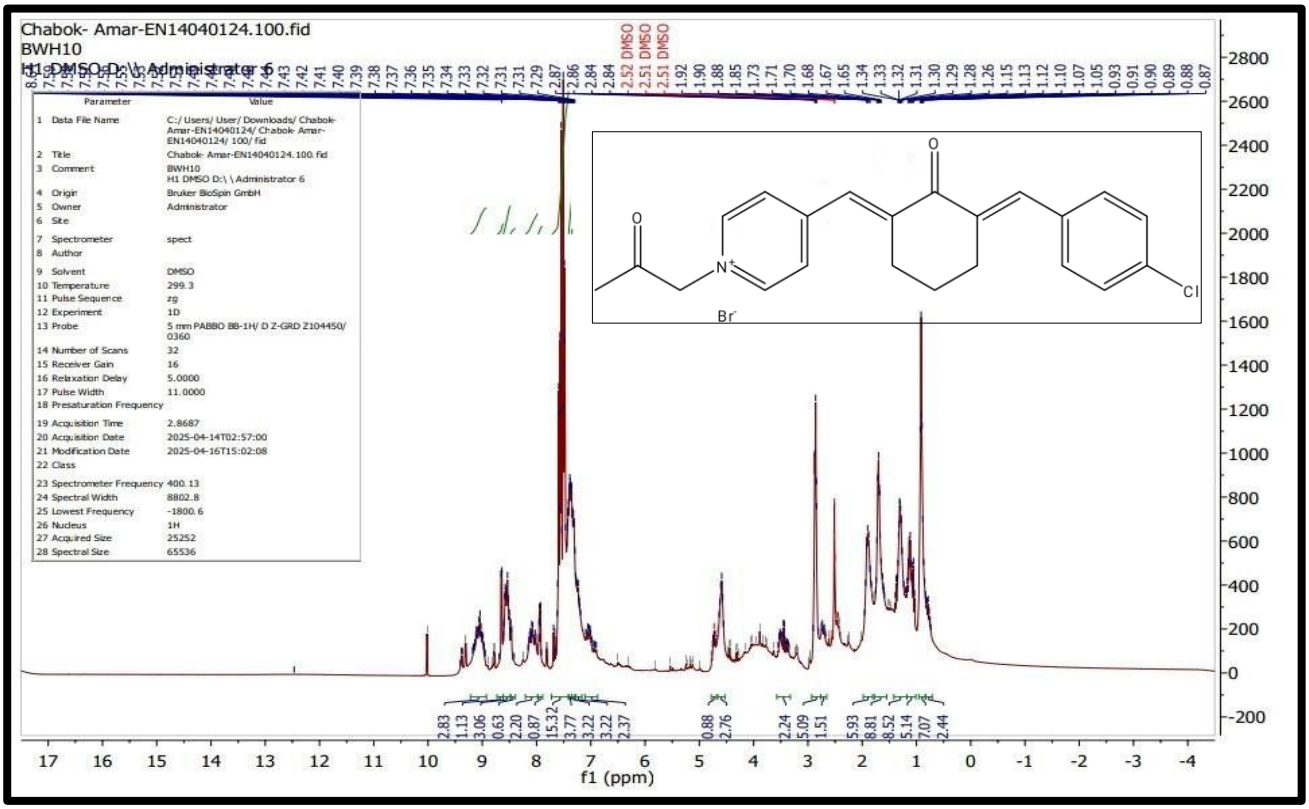

Figure 8. [1]H-NMR of compound (C2).

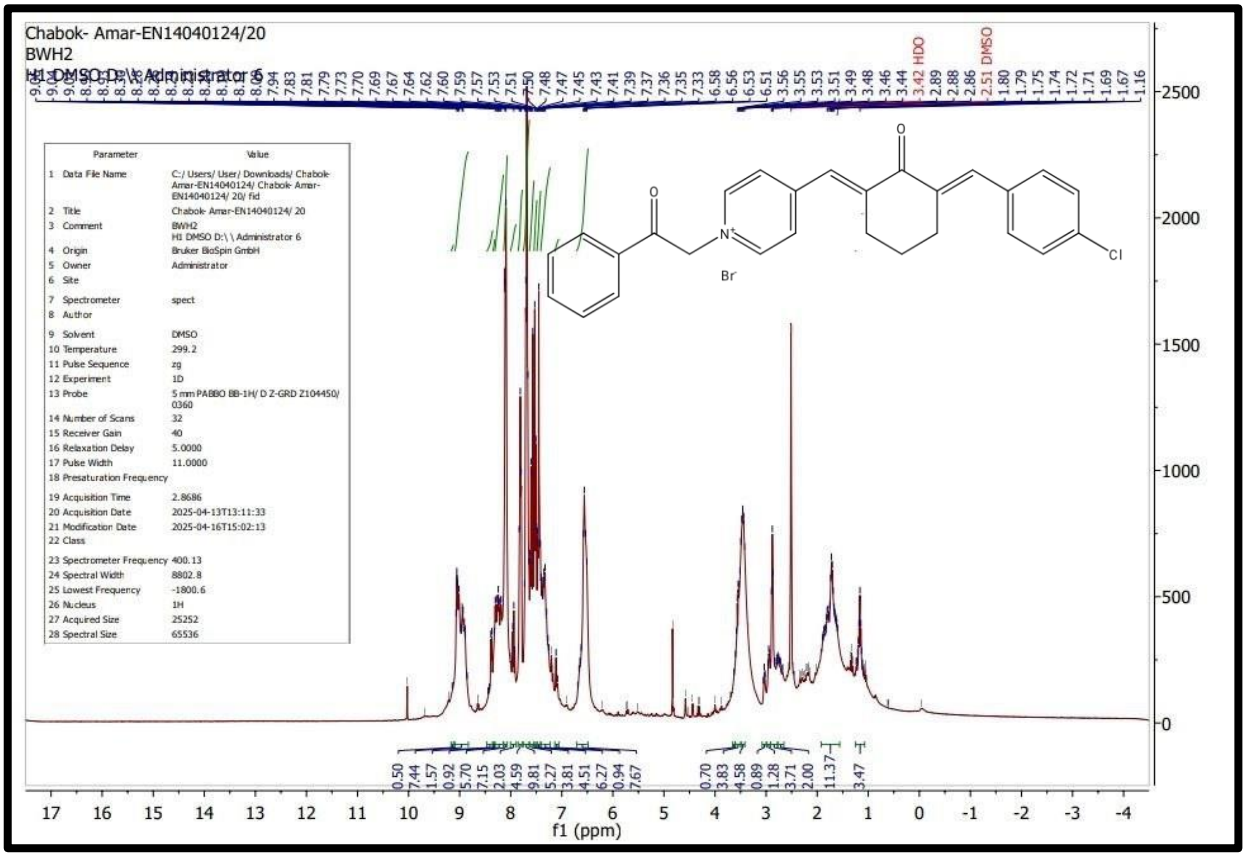

Figure 9. [1]H-NMR of compound (C3).

Table 3. Corrosion rate (**CR**), inhibition efficiency (**IE% %**), surface coverage (**Θ**), and standard absorption energy (**ΔG^{o}_{ads}**) of the inhibitors in 1M H_2SO_4 solution

Concentration (M)	Corrosion rate ($mg.cm^{-2.\,h-1}$)	IE%	θ	K_{ads}	ΔG^{o}_{ads} (kJ. mol^{-1})
Blank	4.263694				
(C1)					
0.0005	0.10743	97.4803	0.9748	0.00001354	-37.7232 R^2=0.999
0.001	0.07261	98.2969	0.9829		
0.005	0.02675	99.37	0.9937		
0.01	0.0178	99.58	0.998		
(C2)					
0.0005	0.0603	98.5858	0.98586	0.00000621	-39.1698 R^2=0.999
0.001	0.04034	99.0538	0.99054		
0.005	0.02081	99.5119	0.99512		
0.01	0.01699	99.6016	0.99602		
(C3)					
0.0005	0.07983	98.1276	0.981276	0.00000755	-39.1703 R2=0.999
0.001	0.047134	98.8945	0.988945		
0.005	0.024204	99.4323	0.994323		
0.01	0.02081	99.5119	0.995119		

RESULTS AND DISCUSSION

Table 3 provides the weight loss data for mild steel exposed to 1 M H_2SO_4 in both the presence and absence of inhibitors at various concentration levels. According to the data in the table, the corrosion rate is greatest in the uninhibited solution. But when inhibitors are added, the corrosion rate is reduced noticeably and gradually [17]. The percentage of inhibition efficiency rises with an increase in the concentration of inhibitors. All inhibitors exhibit maximal inhibitory efficiency at a concentration of 0.01 M. The findings further suggest that the performance of the inhibitors (C1–C3) was almost equivalent [18–20]. This indicates that as the inhibitor concentration increases, a higher number of inhibitor molecules become adsorbed onto the mild steel surface, resulting in the formation of a protective layer. The formation of this barrier layer limits the access of corrosive agents to the metal surface, thus diminishing or preventing corrosion [21]. The adsorption equation is a valuable and important tool for understanding the nature of the interaction between inhibitor molecules and the metal surface. The adsorption mechanism of an inhibitor is usually explained using an adsorption isotherm. In particular, the plots of C_{inh}/θ vs C_{inh} (Fig. 10) gave a straight line with a correlation coefficient near 1(0.999) for inhibitors, indicating that their adsorption onto the MS surface conforms to Langmuir's adsorption isotherm, expressed by the subsequent equation, and the value of Kads was calculated from the intercept [22] (See figure 10).

$$C/\theta = (1/Kads) + C \quad (3)$$

Where C refers to the inhibitor concentration expressed in ppm, Θ is surface coverage, and K_{ads} is the equilibrium constant. The surface coverage (θ) of Pyridinium salts on the metal surface across all approaches was determined using inhibitory efficiency values based on the following equation [23]:

$$\theta = \frac{IE\%}{100} \quad (4)$$

The standard adsorption free energy (ΔG^0_{ads}) depends on K_{ads} and can be calculated by using the following equation [24].

$$\Delta G^{\circ} ads = -RT\ ln\ ln\ (55.5\ Kads) \quad (5)$$

Where R denotes the universal gas constant (8.314 $J{\cdot}mol^{-1}{\cdot}K^{-1}$), while 55.5 represents the molar concentration of water in aqueous solution ($mol{\cdot}L^{-1}$), and T is the system temperature.

The negative values of three inhibitors demonstrated their spontaneous adsorption on the metal surface in 1M H_2SO_4. The value of ΔGo ads is utilized to ascertain the nature of the adsorption process. The results from this investigation indicate that the ΔG^{o}_{ads} value ranges from -20 kJ.mol^{-1} to -40 kJ.mol^{-1}. This range signifies the simultaneous presence of chemisorption and physisorption mechanisms [25, 26]. Inhibitor compounds contain positively charged nitrogen atoms that adsorb onto the negatively charged OH^- ions present in the surrounding environment through electrostatic interactions. Moreover, the π-electrons of the aromatic ring and the lone electron pairs on the oxygen atom of the carbonyl group enable the creation of coordination bonds with the unoccupied d-orbitals of the iron atoms on the metal surface, thus adhering chemically to the surface. Both chemical and physical adsorption act together to protect the metal surface from the harmful effects of the acidic corrosive environment [27]. The order of inhibition efficiency for the synthesized compound is: C2>C3>C1.

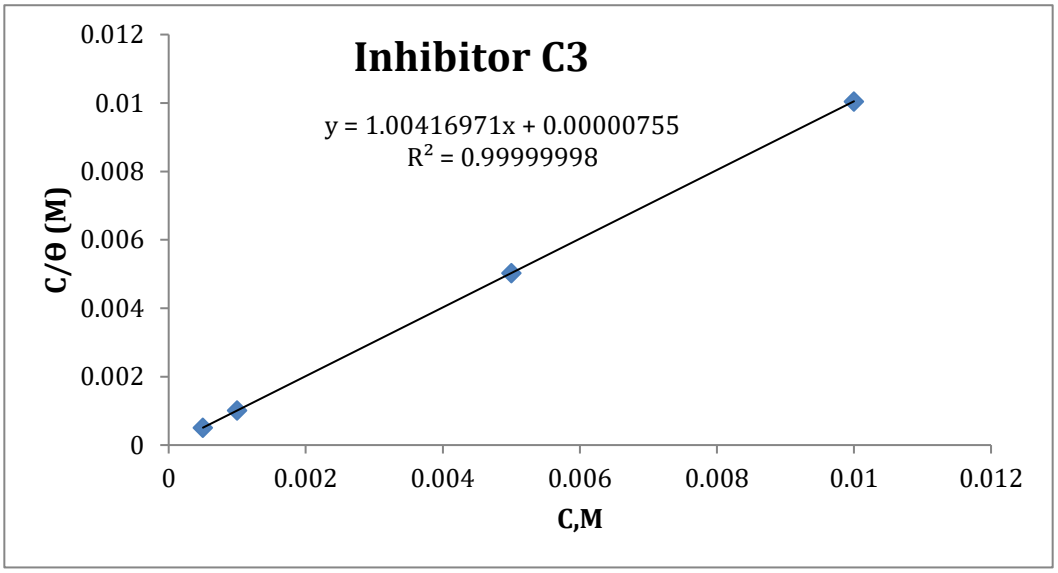

Figure 10. The linear relationship between C/θ versus C for (C3).

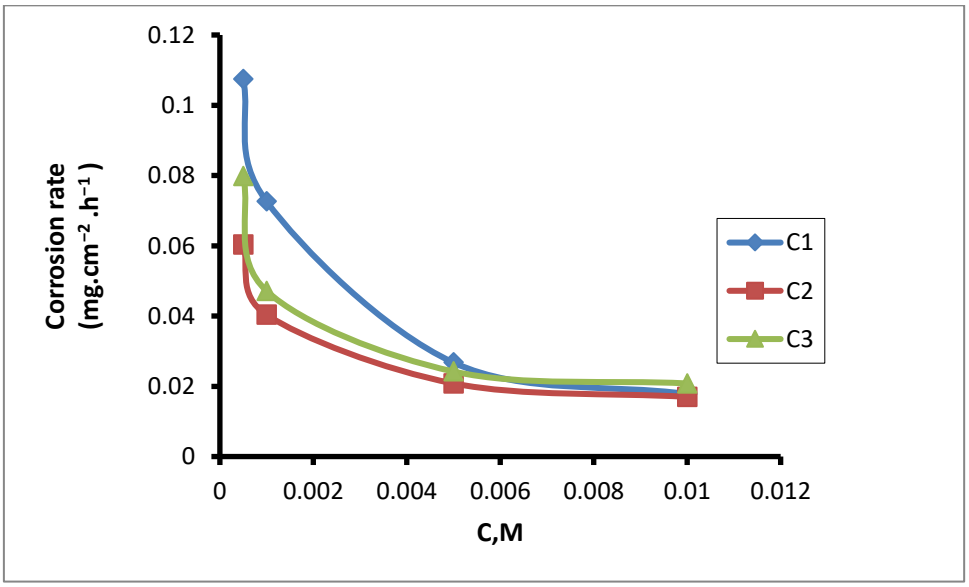

Figure 11. Effect of concentration of inhibitors on mild steel corrosion rate in 1 M H_2SO_4 with the suggested inhibitors (C1, C2, and C3).

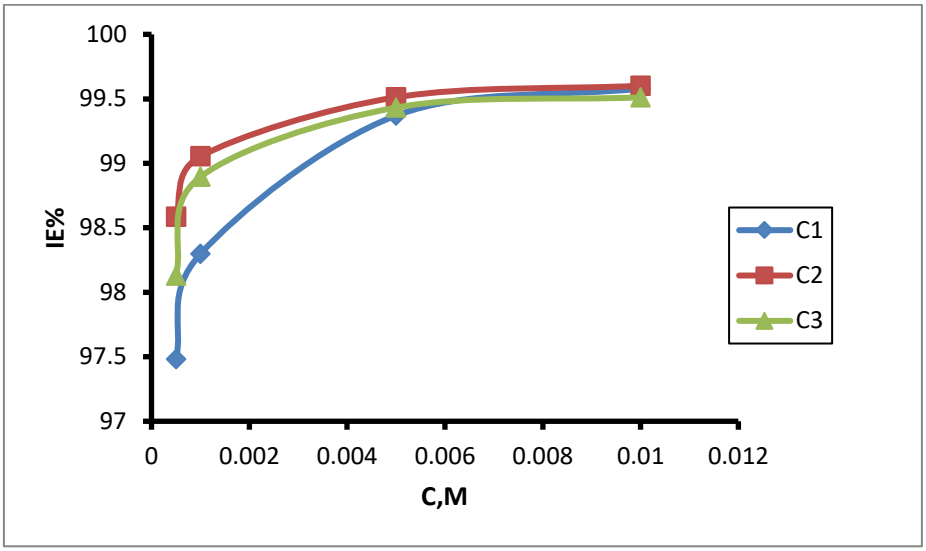

Figure 12. Effects of different concentrations of inhibitors on the effectiveness of inhibiting mild steel in 1 M H_2SO_4 with the suggested inhibitors (C1, C2, and C3).

CONCLUSION

The inhibition effectiveness of mild steel corrosion in 1M sulfuric acid by three synthesized pyridinium salts was systematically evaluated using the traditional weight loss method. An elevation in inhibitor concentration led to augmented inhibition efficiency, a reduction in the corrosion rate, and enhanced surface coverage of the steel substrate. The adsorption behavior of the inhibitors was consistent with a mixed mechanism, involving contributions from both physical and chemical adsorption. Overall, these findings confirm that pyridinium salts are effective candidates for protecting mild steel against acid corrosion, and their performance improves in a concentration-dependent manner.

CONFLICT OF INTEREST

I declare that there are no conflicts of interest.

ACKNOWLEDGEMENTS

I would like to express my sincere gratitude to all those who supported me throughout this work, especially my supervisor, colleagues, and family.

REFERENCES

1. Abd El-Lateef, H., Ismael, M., and Mohamed, I. (2015). Novel Schiff base amino acid as corrosion inhibitors for carbon steel in CO2-saturated 3.5% NaCl solution: experimental and computational study. *Corrosion Reviews*, **33**, 77–97.

2. Sherif, E. S. (2014). A comparative study on the electrochemical corrosion behavior of iron and X-65 steel in 4.0 wt% sodium chloride solution after different exposure intervals. *Molecules*, **19,** 9962–9974.

3. Annon, I., Jlood, K., Hanoon, M., Sayyid, F., Al-Azzawi, W., and Al-Amiery, A. (2024). Corrosion inhibition of mild steel in HCL solution using MPO: Experimental and theoretical insights. *Journal of Materials and Engineering*, **2**, 104–118.

4. Zamindar, S., Mandal, S., Murmu, M., and Banerjee, P. (2024). Unveiling the future of steel corrosion inhibition: a revolutionary sustainable odyssey with a special emphasis on N+-containing ionic liquids through cutting-edge innovations. *Materials Advances*, **5**, 4563–4600.

5. Pavelyev, R., Zaripova, Y., Yarkovoi, V., Vinogradova, S., Razhabov, S., Khayarov, K., Nazarychev, S., Stoporev, A., Mendgaziev, R., Semenov, A., Valiullin, L., Varfolomeev, M., and Kelland, M. (2020). Performance of waterborne polyurethanes in inhibition of gas hydrate formation and corrosion: Influence of hydrophobic fragments. *Molecules*, **25**, 5664.

6. Nahlé, A., Salim, R., Hajjaji, F., Ech-Chihbi, E., Titi, A., Messali, M., Kaya, S., El Ibrahimi, B., and Taleb, M. (2022). Experimental and theoretical approach for novel imidazolium ionic liquids as Smart Corrosion inhibitors for mild steel in 1.0 M hydrochloric acid. *Arabian Journal of Chemistry*, **15**, 103967.

7. Wang, C., Chen, J., Hu, B., Liu, Z., Wang, C., Han, J., Su, M., Li, Y., and Li, C. (2019). Modified chitosan-oligosaccharide and sodium silicate as efficient, sustainable inhibitor for carbon steel against chloride-induced corrosion. *Journal of Cleaner Production*, **238**, 117823.

8. Luo, F., Yao, P., Zhang, J., and Li, E. (2025). Alkyl pyridine ionic liquid as a green corrosion inhibitor for mild steel in acidic medium. *RSC advances*, **15**, 27369–27387.

9. Ahmed, M., Amin, S., and Mohamed, A. (2024). Current and emerging trends of inorganic, organic, and eco-friendly corrosion inhibitors. *RSC advances*, **14**, 31877–31920.

10. Boutaqqa, O., Ettahiri, W., Adardour, M., Safir, E., Alanazi, A., Naamane, S., Rais, Z., Baouid, A., Wiedmer, S., and Taleb, M. (2025). Synthesis and assessment of benzimidazole derivatives as effective corrosion inhibitors for mild steel in acidic environments: an experimental and theoretical approach. *Journal of Molecular Structure*, **1347**, 143281.

11. Syam, S., Abdelwahab, S., Al-Mamary, M., and Mohan, S. (2012). Synthesis of chalcones with anticancer activities. *Molecules*, **17**, 6179–6195.

12. Pulipati, S., Babu, P., Kausar, S., Sani, S., Hima, K., Bindu, A., and Jyothirmayee, N. (2018). Synthesis and evaluation of antibacterial activity of benzal and its derivatives. *Inventi Rapid: Med. Chem.*, **4**, 1–6.

13. Ahmed, M., and Shihab, M. (2023). Pyridinium bromide derivatives as corrosion inhibitors for mild steel in 1M H2SO4. *Egyptian Journal of Chemistry*, **66**, 63–72.

14. Cai, C., Yu, C., Taryba, M., Alves, M., Song, R., Cui, Y., and Montemor, M. (2025). Revealing the early electrochemical corrosion behavior of Mg–Zn–Zr-Nd alloys in a simulated orthopedic environment. *Journal of Materials Research and Technology*, **35**, 4217–4230.

15. Aslam, J., Aslam, R., Alrefaee, S., Mobin, M., Aslam, A., Parveen, M., and Hussain, C. (2020). Gravimetric, electrochemical, and morphological studies of an isoxazole derivative as a corrosion inhibitor for mild steel in 1M HCl. *Arabian Journal of Chemistry*, **13**, 7744–7758.

16. Kumari, P. and Lavanya, M. (2021). Optimization of inhibition efficiency of a Schiff base on mild steel in an acid medium: electrochemical and RSM approach. *Journal of Bio-and Tribo-Corrosion*, **7**, 110.

17. Sakki, B., Said, M., Mezhoud, B., Allal, H., Larbah, Y., Kherrouba, A., Chibani, A., and Bouraiou, A. (2022). Experimental and theoretical study on corrosion inhibition of pyridinium salts derivatives for API 5L Gr. B steel in acidic media. *Journal of Adhesion Science and Technology*, **36,** 2245–2268.

18. Raheem, A. A., Shihab, M. S. (2022). Synthesis and study behavior of some new pyridinium salts as corrosion inhibitors for mild steel in 1m H_2SO4. *Al-Nahrain J. Sci.*, **25(4)**, 21–31.

19. Muhsin, M., and Shihab, M. (2023). Synthesis of New Triethylammonium Salts as Corrosion Inhibitors for Mild Steel in 1 M H_2SO4. *Al-Nahrain Journal of Science*, **26**, 6–18.

20. Kareem, R., and Shihab, M. (2021). Study new pyridine derivatives as corrosion inhibitors for mild steel in an acidic media. *Al-Nahrain Journal of Science*, **24**, 1–8.

21. Abeng, F. and Anadebe, V. (2023). Combined electrochemical, DFT/MD-simulation, and hybrid machine learning based on ANN-ANFIS models for prediction of doxorubicin drug as corrosion inhibitor for mild steel in 0.5 M H_2SO4 solution. *Computational and Theoretical Chemistry*, **1229**, 114334.

22. Belal, K., El-Askalany, A., Ghaith, E., and Molouk, A. (2025). A comprehensive experimental and theoretical perspective of novel triazole-based pyridine and quinoline derivatives for corrosion protection of carbon steel in sulfuric acid solution. *Scientific Reports*, **15**, 26938.

23. Kumar, B., Vashisht, H., Goyal, M., Kumar, A., Benhiba, F., Prasad, A.K., Kumar, S., Bahadur, I., and Zarrouk, A. (2020). Study of adsorption mechanism of chalcone derivatives on mild steel-sulfuric acid interface. *Journal of Molecular Liquids*, **318**, 113890.

24. Ogunleye, O., Arinkoola, A., Eletta, O., Agbede, O., Osho, Y., Morakinyo, A., and Hamed, J. (2020) Green corrosion inhibition and adsorption characteristics of Luffa cylindrica leaf extract on mild steel in hydrochloric acid environment. *Heliyon*, **6.**

25. Hassan, H., Rashid, K., AL-Azawi, K., and Khadom, A. (2024). A combined experimental and theoretical study into the effect of a new heterocyclic compound containing β-lactam ring as corrosion inhibitor for mild steel in hydrochloric acid. *Results in Surfaces and Interfaces*, **17**, 100319.

26. Iroha, N., Maduelosi, N., and Nnanna, L. (2023). The impact of tizanidine on E24 carbon steel corrosion inhibition in oilfield acidizing solution: experimental and quantum chemical studies. *Emergent Materials*, **6,** 137–146.

27. Öztürk, S., Gece, G., Yıldırım, A. and Gerengi, H. (2023). Newly synthesized pyridinium salt based tricationic surfactants as corrosion inhibitor for carbon steel in 1.0 m HCl medium. *Protection of Metals and Physical Chemistry of Surfaces*, **59**, 750–762.